

Terahertz imaging with self-pulsations in quantum cascade lasers under optical feedback

Cite as: APL Photonics 6, 091301 (2021); <https://doi.org/10.1063/5.0056487>

Submitted: 11 May 2021 • Accepted: 15 August 2021 • Published Online: 01 September 2021

 Xiaoqiong Qi,  Karl Bertling,  Thomas Taimre, et al.



View Online



Export Citation



CrossMark

ARTICLES YOU MAY BE INTERESTED IN

[Efficient photoconductive terahertz detection through photon trapping in plasmonic nanocavities](#)

APL Photonics 6, 080802 (2021); <https://doi.org/10.1063/5.0055332>

[Dielectric slot-coupled half-Maxwell fisheye lens as octave-bandwidth beam expander for terahertz-range applications](#)

APL Photonics 6, 096104 (2021); <https://doi.org/10.1063/5.0054251>

[High-pulse-energy III-V-on-silicon-nitride mode-locked laser](#)

APL Photonics 6, 096102 (2021); <https://doi.org/10.1063/5.0058022>



THE ADVANCED MATERIALS MANUFACTURER

yttrium iron garnet glassy carbon beamsplitters fused quartz additive manufacturing
 zeolites III-IV semiconductors gallium lump copper nanoparticles organometallics
 nano ribbons barium fluoride europium phosphors photonics infrared dyes
 epitaxial crystal growth ultra high purity materials transparent ceramics CIGS
 cerium oxide polishing powder surface functionalized nanoparticles MRE grade materials thin film
 silver nanoparticles perovskites OLED lighting solar energy
 rare earth metals quantum dots sputtering targets fiber optics
 osmium scintillation Ce:YAG h-BN deposition slugs
 refractory metals laser crystals CVD precursors photovoltaics
 anode lithium niobate InAs wafers metamaterials borosilicate glass
 dysprosium pellets MOFs AuNPs YBCO superconductors InGaAs
 chalcogenides ZnS CdTe indium tin oxide MgF2 rutile
 perovskite crystals transparent ceramics diamond micropowder optical glass

The Next Generation of Material Science Catalogs



Terahertz imaging with self-pulsations in quantum cascade lasers under optical feedback

Cite as: APL Photon. 6, 091301 (2021); doi: 10.1063/5.0056487

Submitted: 11 May 2021 • Accepted: 15 August 2021 •

Published Online: 1 September 2021



View Online



Export Citation



CrossMark

Xiaoqiong Qi,¹ Karl Bertling,¹ Thomas Taimre,² Yah Leng Lim,¹ Tim Gillespie,¹ Paul Dean,³ Lian He Li,³ Edmund H. Linfield,³ A. Giles Davies,³ Dragan Indjin,³ and Aleksandar D. Rakić^{1,a)}

AFFILIATIONS

¹School of Information Technology and Electrical Engineering, The University of Queensland, Brisbane, Queensland 4072, Australia

²School of Mathematics and Physics, The University of Queensland, Brisbane, Queensland 4072, Australia

³School of Electronic and Electrical Engineering, University of Leeds, Leeds LS2 9JT, United Kingdom

^{a)}Author to whom correspondence should be addressed: a.rakic@uq.edu.au

ABSTRACT

The phenomenon of self-pulsation (SP) in terahertz (THz) quantum cascade lasers (QCLs) due to optical feedback was reported recently. In this Letter, we propose a THz imaging modality using the SP phenomenon in a THz QCL. We explore the theoretical oscillation properties of the SP scheme and demonstrate its suitability to perform imaging experimentally. The SP imaging scheme operates in self-detection mode, eliminating the need for an external detector. Moreover, the scheme requires only a fixed current, meaning that one can avoid many of the pitfalls associated with high temperature operation of THz QCLs, including frequency chirp and mode hops caused by sweeping the laser current. This also means that one is free to locate the operating point at the maximum power, to produce the desired beam profile or for highest spectral purity, depending on the application. The SP imaging modality proposed in this work can be translated directly to high operating temperature THz QCLs.

© 2021 Author(s). All article content, except where otherwise noted, is licensed under a Creative Commons Attribution (CC BY) license (<http://creativecommons.org/licenses/by/4.0/>). <https://doi.org/10.1063/5.0056487>

The past two decades have witnessed the most significant effort to utilize the terahertz (THz) spectrum,^{1,2} with the THz quantum cascade lasers (QCLs) emerging as, arguably, the most promising high power source^{3–6} and even a coherent detector^{7–10} for applications in THz imaging. Yet, this difficult-to-tame part of the electromagnetic spectrum, with some unique qualities, and the associated QCL still have to deliver on the promises made long ago. One of the long-standing issues is obvious: since their inception, THz QCLs have been associated with cryogenic cooling and efficient operation at ultra-low temperatures. Second, the THz detectors are not sensitive or fast enough, which further limits the application of THz technology in a wide range of areas.^{11,12}

As a self-detection technique, THz imaging using self-mixing (SM) in THz QCLs under optical feedback (OF) has witnessed increased interest over the last decade in a wide variety of areas,

including chemical sensing, materials analysis, and high-resolution spectroscopy.^{7,10,13–16} SM imaging is a highly coherent and self-alignment imaging technique where the laser itself acts as a high speed and highly sensitive detector. However, in order to create a time-varying SM signal, the SM scheme for imaging or sensing typically requires modulation of laser current or modulation of external cavity parameters, such as target movement or changing target reflectivity⁸ (with exception¹⁴). Emission frequency sweeping through driving current modulation is widely used in THz QCL based SM imaging systems with a static target.^{10,16,17} This imposes a demanding requirement for the current range at which the laser operates, i.e., the lasers' dynamic working range, especially for high temperature operation of THz QCLs.

High temperature operation of THz QCLs in pulsed mode at ~250 K has been demonstrated recently by Khalatpour *et al.*,⁶ which

is contrary to the long-held belief that THz QCLs are associated with cryogenic cooling and efficient operation at ultra-low temperatures. This work shows that room-temperature operation of THz QCL is indeed possible. This comes after recent advances detailed in Refs. 4 and 5. However, with the increase in temperature, the lasers' dynamic working range is significantly reduced. At higher temperatures, the light-current curves peak sharply at a single current.⁶ To make the most of such a laser for sensing and imaging applications, one therefore needs a scheme that can operate solely at this peak output power.

The self-pulsation (SP) phenomenon that we have recently observed in THz QCLs, as illustrated in Fig. 1, can be used for harnessing the potential of this laser. We have experimentally observed and theoretically explained SP in THz QCLs under OF,¹⁸ in contrast to the generally accepted claim that THz QCLs are ultrastable against feedback.^{19,20} Periodic pulsations appear at frequencies that can be associated with the round-trip time in the external cavity τ_{ext} . Even if the laser is turned on for a very short duration of time (a few hundreds of ns), a number of these pulses are detected in the emitted power or terminal voltage of the laser.

In this Letter, we propose a THz imaging modality using the SP phenomenon in a THz QCL. Both the amplitude and the fundamental frequencies of the SPs are monotonically increasing with the feedback coupling coefficient, which is the fundamental principle of the imaging modality we proposed in this work. We explore the oscillation properties of the SP scheme and demonstrate the SP imaging scheme experimentally. In this SP scheme, the THz QCL is driven by a square current pulse—a fixed current—that is effective in producing THz images at high frame-rate and can be translated directly to forthcoming room temperature devices. Considering that the detection scheme proposed in this work requires only a fixed current, undesirable mode hops, frequency chirp, and evolution of the beam profile during the driving current sweep are eliminated. One is then free to locate the operating point at the maximum power, to produce the desired beam profile or for highest spectral purity,

depending on the application. A number of issues with high temperature operation, including that the lasers' dynamic working range reduces with increasing operation temperature and the light-current curves peak sharply at a single current at higher temperatures, have been pointed out in Refs. 6 and 21; however, most of them are common to all QCLs (regardless of the operating temperature), and none of them would prevent the successful usage of our sensing and imaging scheme.

The SP dynamics and the system used for THz imaging with the SP phenomenon in the single-mode THz QCL is shown in Fig. 1. The laser was driven by a square pulse I [Fig. 1(a)], and the laser beam emitted from the QCL is collimated by a collimating lens and focused by an objective lens before incidence upon a target [Fig. 1(b)]. The reflected light from the target is re-injected into the laser cavity where it mixes with the intra-cavity electric field and creates periodic pulsations of the emission power P_{out} and population inversion ΔN , where the driving pulse duration is on the same order of the duration of the SPs [as shown by simulated SP dynamics in Fig. 1(a), the dynamics during turn-on delay τ_d and the two initial round-trips of the external cavity are to be ignored]. The time spacing between two adjacent SPs is around the external cavity round-trip delay time τ_{ext} . The SP waveforms of P_{out} and ΔN are out of phase. Theoretically, we study the OF induced dynamics through the emission power or population inversion, which can be directly solved from a set of reduced-rate equations (RREs).^{18,22} Experimentally, we observe the laser terminal voltage V (which is determined by population inversion) without the need for THz photodetectors. The QCL itself acts as a high speed and highly sensitive detector.

The variations of the amplitude and the frequency of the SPs are dependent on the C parameter, which is defined as $C = (\kappa/\tau_{\text{in}})\tau_{\text{ext}}\sqrt{1 + \alpha^2}$, where $\kappa = \epsilon\sqrt{R/R_2}(1 - R_2)$ is the feedback coupling coefficient, τ_{in} is the laser cavity round-trip time, and α is the linewidth enhancement factor of the laser.¹⁰ Since κ contains the information of the optical properties of the target (re-injection

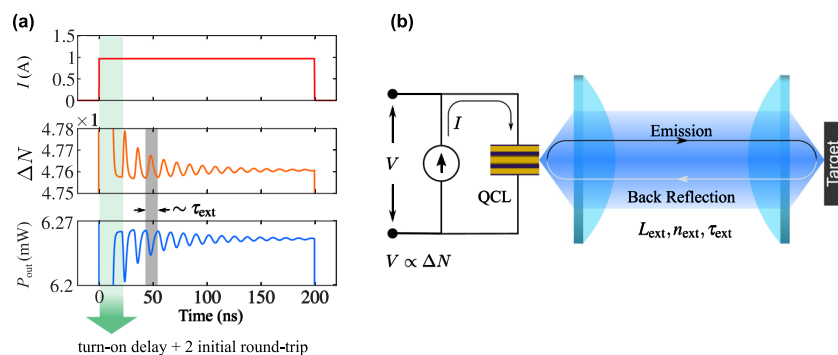


FIG. 1. The SP dynamics and the system used for THz imaging with the SP phenomenon in the THz QCL: (a) The driving current I , population inversion ΔN , and emission power P_{out} of the THz QCL. The laser was driven by a square pulse I ; (b) the system used for THz imaging with the SP phenomenon in the THz QCL. The laser beam emitted from the QCL is collimated by a collimating lens and focused by an objective lens before incidence upon a target. The reflected light from the target is re-injected into the laser cavity where it mixes with the intra-cavity electric field and induces periodic pulsations into the emission power P_{out} and population inversion ΔN , where the driving pulse duration is on the same order of the duration of the SPs [as shown by simulated SP dynamics in (a), the dynamics during turn-on delay and the two initial round-trips of the external cavity are to be ignored]. The quantities L_{ext} , n_{ext} , and τ_{ext} are the length, refractive index, and round-trip time of the external laser cavity, respectively. The time spacing between two adjacent SPs is around the external cavity round-trip delay time τ_{ext} . The optical characteristics of the target are imprinted on the variations in amplitudes and frequencies of the SPs during a raster scan of the target, which can be extracted by an FPGA based control board and used to reconstruct the target image.

coupling coefficient ϵ , reflectivity of the target R , and the exit laser facet reflectivity R_2), the optical characteristics of the target are imprinted on the variations in amplitudes and frequencies of the SPs during a raster scan of the target, which can be extracted by a field-programmable gate array (FPGA) based control board and used to reconstruct the target image.

In order to demonstrate the periodic oscillation properties of the SP phenomenon in the THz QCL under all OF levels, we solved the emission power and the phase of the slowly varying envelope of the electric field from the theoretical model of the system, which is the set of RREs with OF terms as described in Ref. 18. The parameters of the system are also consistent with those used in that work unless otherwise specified. We simulate the emission power from the THz QCL with increasing OF strength. Figure 2 demonstrates the influence of OF strength on laser dynamics in a THz QCL with an external cavity length of 1.6 m.

The time evolution of the emitted power, emission spectra offset from the free-running emission frequency, and the slowly varying envelope field phasor (real part vs imaginary part of the electric field) with the re-injection coupling factor ϵ at -90 , -60 , -30 , and 0 dB are shown in each column of Fig. 2, respectively. In the case of free-running THz QCL without OF (not shown here),

the emission power reaches its steady-state after a turn-on delay τ_d . The value of τ_d depends on the carrier lifetimes, driving current, and the gain factor of the THz QCL, which is typically ten times smaller than that in a laser diode (LD) due to ultrashort carrier lifetimes in THz QCLs.²² In this particular device, τ_d is around 200 ps. When the THz QCL is subject to OF, although τ_d remains unchanged, a laser transient oscillation starts from $\tau_d + \tau_{ext}$ due to the delayed arrival of emitted optical power from the target. The value of τ_{ext} is on the ns time scale when the external cavity is several meters long; here, it is 10.67 ns with an external cavity length of 1.6 m. As shown in Fig. 2(a1), there is a sudden change in power at $\tau_d + \tau_{ext}$ when ϵ is -90 dB. The short time transient dynamics under weak feedback does not change the emission spectrum and the phasor is essentially a fixed point, as shown in Figs. 2(a2) and 2(a3), respectively. However, although only an on-off emission power change is visible when ϵ is -60 dB in Fig. 2(b1), the phase starts shifting due to increased feedback in this case. Consequently, the linewidth is broadened in Fig. 2(b2), and the phasor transitions to be a partial circle with the direction indicated by the arrow in Fig. 2(b3). When ϵ is even stronger at -30 dB, the emission power starts varying periodically with a period of around τ_{ext} and the amplitude of this oscillation is around

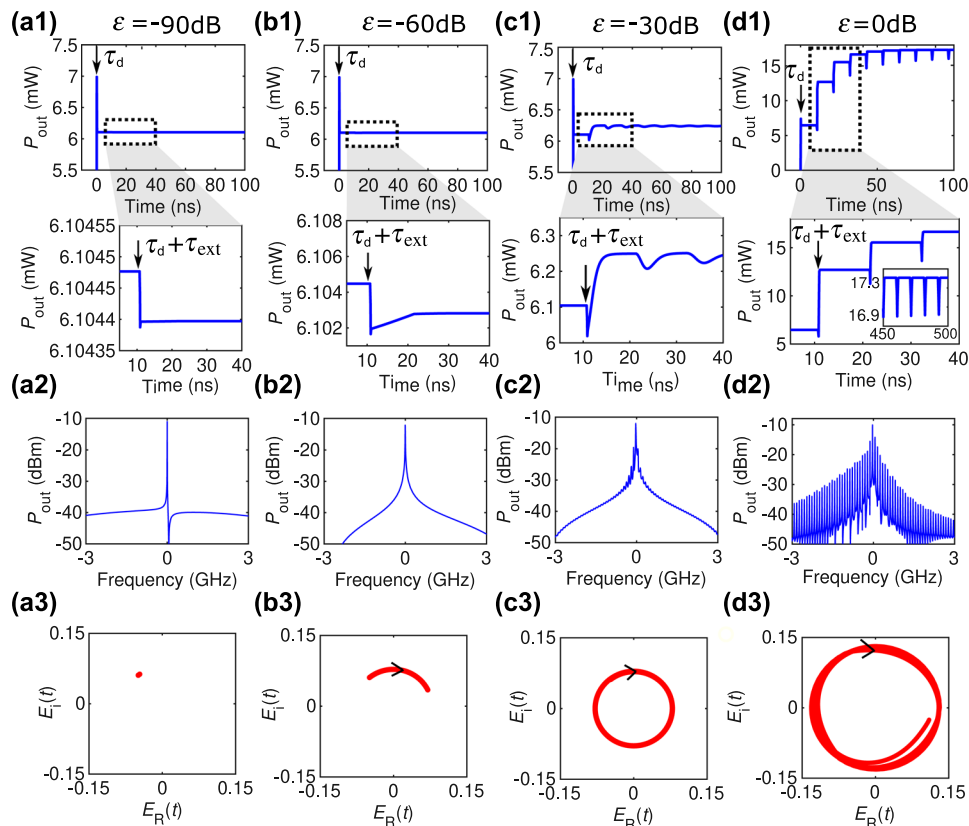


FIG. 2. Simulated emission power time evolution (row 1) from the THz QCL with a zoomed-in view of feedback dynamics (row 2), emission spectrum offset to the emission frequency (row 3), and the phasor plots (row 4) from a single-mode THz QCL under OF with increasing feedback strengths, where the external cavity length $L_{ext} = 1.6$ m: (a) $\epsilon = -90$ dB, $\kappa = -89.04$ dB, $C = 0.0086$; (b) $\epsilon = -60$ dB, $\kappa = -59.04$ dB, $C = 0.27$; (c) $\epsilon = -30$ dB, $\kappa = -29.04$ dB, $C = 8.60$; and (d) $\epsilon = 0$ dB, $\kappa = 0.96$ dB, $C = 272.06$.

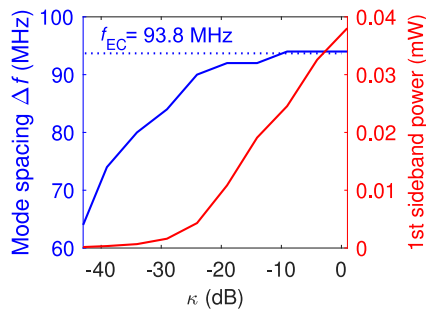


FIG. 3. Simulated dependence of mode spacing Δf and the first right sideband power in the emission spectrum of Fig. 2 on the feedback coupling coefficient κ , where $L_{\text{ext}} = 1.6$ m.

0.04 mW in Fig. 2(c1). Accordingly, the emission spectrum exhibits multiple external cavity modes with the mode spacing defined as Δf [Fig. 2(c2)]. The phasor extends into a complete circle in a clockwise direction [Fig. 2(c3)]. Furthermore, in order to explore laser dynamics in the THz QCL under the strongest feedback condition, the simulation with ϵ of 0 dB, corresponding to 100% OF into the laser cavity, was performed. The results are shown in Fig. 2(d). The periodic power oscillation amplitude is further increased to 4.2 mW at 20 ns and 0.4 mW at 500 ns [see zoomed-in view of Fig. 2(d1)]. The number of sidebands is significantly enhanced with the increase in feedback strength [Fig. 2(d2)]. However, the phasor is still a circle due to the periodic oscillation nature of the emission power, with increased circle radius [Fig. 2(d3)]. It should be noted that the waveform of the SPs is dependent on the feedback phase as demonstrated in Ref. 18. We confirmed in this work that no chaotic oscillations were observed from the phasor even under this extreme level of OF. These simplified OF dynamics in THz QCLs make them very suitable to be used for sensing and imaging.

Mode spacing Δf in the emission spectrum (frequency splitting) of Fig. 2 or the oscillation frequency of the SPs increases with increasing feedback strength and exhibits a frequency modulation property, as shown in Fig. 3 (blue curve). The value of Δf asymptotically tends to equal the external cavity resonant frequency $f_{\text{EC}} = c/(2n_{\text{ext}}L_{\text{ext}})$ (where c is the speed of light in a vacuum and n_{ext} and L_{ext} are the refractive index and length of the external cavity, respectively) at 93.8 MHz, as marked by the blue dashed line in Fig. 3. In addition, the amplitude of the multiple external cavity modes in the emission spectrum also increases with the increasing feedback strength due to more power being returned to the laser cavity. The amplitude of the first split frequency at the right side of the central

emission frequency is plotted as a function of κ in Fig. 3 (red curve). Both the amplitude and the fundamental frequencies of the SPs are monotonically increasing with the feedback coupling coefficient κ , which is the fundamental principle of the imaging modality we proposed in this work. The amplitude and the fundamental frequencies of the SPs could be used as a sensing and imaging signal to measure the parameters in the feedback coupling coefficient κ , which includes the re-injection coupling factor, reflectivity of the external target, internal reflection coefficient of emitting laser facet, as well as the linewidth enhancement factor of the laser.

A pulsed-mode THz QCL under OF as shown in Fig. 1(b) was used to observe the SPs experimentally. The QCL consisted of a 12 μm -thick AlGaAs/GaAs nine-well phonon-assisted active region.²³ Starting from the injection barrier, the layer sequence for each of the 95 periods is 4/10.1/0.5/16.2/1/12.9/2/11.8/3/9.5/3/8.6/3/7.1/3/17/3/14.5 nm (AlGaAs layers are shown in bold, and the 17 nm well is Si-doped by $n = 2 \times 10^{16}$). The structure was grown by solid-source molecular beam epitaxy on a semi-insulating GaAs substrate, with the active region grown between doped upper 50 nm-thick ($n = 5 \times 10^{18} \text{ cm}^{-3}$) and lower 700 nm thick ($n = 2 \times 10^{18} \text{ cm}^{-3}$) GaAs contact layers. The wafer was processed into 150 μm wide surface-plasmon ridge waveguide structures using photolithography and wet chemical etching, with the substrate thinned to 200 μm . Devices were then mechanically cleaved to define a ridge of length 2 mm. The laser was driven by a custom-built laser pulse driver that consisted of a main controller board with an FPGA controlling the pulse generation and SP signal extraction electronics. The driving current was set as the square current pulse train at 0.97 A. Each of the driving pulse is 450 ns long with the duty cycle rate at 20%. The temperature of the laser was controlled by a compact cryogen-free Stirling cooler,¹² and the operating point of the Stirling engine was set at 50 K.

The laser beam emitted from the THz QCL is collimated by using a Tsurupica plastic lens (Tsurupica-RR-CX-1.5-50-SPS, Broadband, Inc.), attenuated by using a wire grid polarizer (G30-L, Microtech Instruments, Inc.), and focused by an objective lens (Plano-convex lens LPX-TPX-D50.8-F100) before being incident upon a target. The SP signal generated during a raster scan of the target was extracted by the FPGA based control board and used to reconstruct the target image. In the first experiment, the target is a 2-in. gold mirror, which was placed in the collimated path at varying distances from the QCL.

The SPs that were obtained from the laser terminal voltage with two different external cavity lengths L_{ext} of 1.6 and 1.93 m are presented in Figs. 4(a) and 4(b), respectively. The corresponding spectrum of the SPs [obtained via Fast Fourier Transform (FFT)

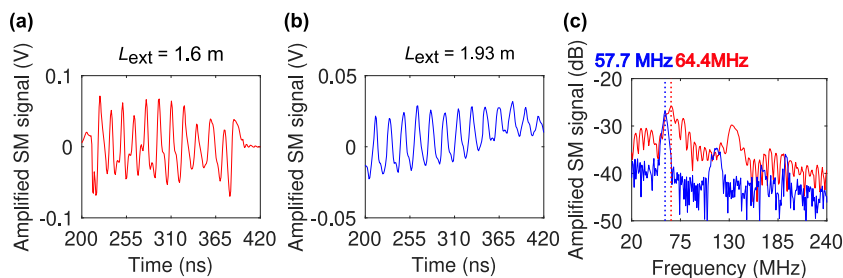


FIG. 4. Experimental observations of the OF dynamics in a THz QCL with a square driving pulse with duration of 450 ns: (a) $L_{\text{ext}} = 1.6$ m; (b) $L_{\text{ext}} = 1.93$ m; and (c) Fourier transform of the SP signal shown in (a) and (b) (red curve: $L_{\text{ext}} = 1.6$ m; blue curve: $L_{\text{ext}} = 1.93$ m).

with the resolution of the spectra is 1 MHz by zero padding the signal] is shown in Fig. 4(c), where the peak frequencies of each spectrum (57.7 and 64.4 MHz) indicate the fundamental frequencies of the SPs for each L_{ext} (1.93 and 1.6 m). The oscillation frequency is expected to reach their maximum values at f_{EC} (93.8 and 78.9 MHz when L_{ext} is 1.6 and 1.93 m, respectively) under 100% OF. However, 100% OF ($\epsilon = 0$ dB) is not likely to be achievable in experiment due to atmospheric absorption and coupling losses both in the forward and return path within the external cavity and practical reflectivity (<100%) of real-world targets. This suggests that the optical feedback level can be improved by increasing the external target reflection, reducing the laser facet reflection by applying antireflection coating^{14,24} and increasing the re-injection coupling factor of the reflected THz beam returning into the laser cavity. A detailed comparison between the simulation and experimental results with different external cavity lengths and feedback strengths can be found in Ref. 18.

In the second experiment, the gold mirror was replaced by a ruler for THz imaging. The face of the ruler was oriented normal to the incident beam, and the image was created by raster scanning the ruler. The external cavity length is 1.6 m in this experiment. As a proof of concept experiment, Fig. 5 displays the THz imaging of a section of a ruler by using the SP phenomenon with a square driving current pulse train. Currently, the image is obtained from the amplitude of the strongest frequency component of the SP oscillations, obtained after an FFT operation on the SP signal from the terminal voltage of the laser. The SP technique is comparable to conventional THz imaging approaches^{8,10,11,13,14} and captures the main features of the target. Both SP and SM imaging techniques are based on self-detection where the laser is used as the high speed and highly sensitive detector. However, SM imaging typically requires modulation of laser current or modulation of external cavity parameters, such as target movement or target reflectivity. In contrast, SP imaging requires only a fixed current, and no modulation of the external cavity parameters is required. Thus, SP imaging is highly suitable for the recently demonstrated THz QCL operating at high temperatures close to 250 K, which has a very limited current operation range and frequency chirp, mode hops, and evolution of the beam profile occurring with current sweep.⁶ Moreover, SM imaging is usually

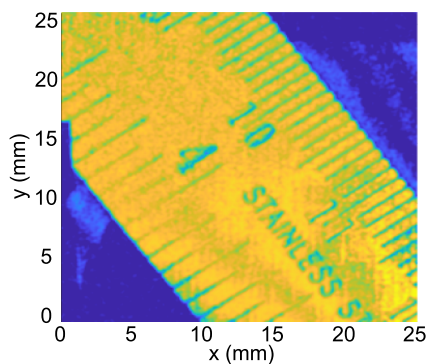


FIG. 5. Experimental THz imaging of a section of a ruler by using self-pulsations with a square driving current pulse train. The image is obtained from the amplitude of the strongest frequency component in the spectrum for each pixel.

operating under weak feedback where the SM signal amplitude is proportional to the feedback coupling coefficient,²⁵ while SP imaging works primarily under moderate and strong feedback conditions where external cavity modes appear and the SP dynamics are clearly pronounced.

In this work, we proposed a new imaging modality for THz QCLs based on the SP phenomenon. This scheme has the distinct benefits of self-detection, which eliminates the need for an external detector, and operates only at a single fixed current, meaning that it is eminently suitable for high temperature devices. We explored the theoretical oscillation properties of the SP scheme and demonstrated its suitability to perform imaging experimentally. This imaging modality is not restricted to THz QCLs and thus presents an opportunity for a range of applications in other parts of the spectrum. The SP dynamics has been reported in mid-infrared QCLs^{20,26,27} and LDs in the short cavity regime.²⁸ Furthermore, the SPs in single-mode THz QCLs investigated in this work also helps the understanding of multi-mode OF dynamics in exotic laser structures, such as in compound cavity lasers,²⁹ or under ultrafast driving current modulation, such as in active mode-locked THz QCLs^{30,31} or random THz QCLs with multiple elastic scattering and rich interference of light wavelets.³²

The authors acknowledge the funding from the Australian Research Council Discovery Project (Grant No. DP200101948) and the Engineering and Physical Sciences Research Council (EPSRC UK) through Grant Nos. EP/J002356/1, EP/P021859/1, and EP/T034246/1. X.Q. acknowledges support from the Advance Queensland Industry Research Fellowships program.

DATA AVAILABILITY

The data that support the findings of this study are available from the corresponding author upon reasonable request.

REFERENCES

- M. Tonouchi, "Cutting-edge terahertz technology," *Nat. Photonics* **1**, 97 (2007).
- S. S. Dhillon, M. S. Vitiello, E. H. Linfield, A. G. Davies, M. C. Hoffmann, J. Booske, C. Paoloni, M. Gensch, P. Weightman, G. P. Williams *et al.*, "The 2017 terahertz science and technology roadmap," *J. Phys. D: Appl. Phys.* **50**, 043001 (2017).
- R. Köhler, A. Tredicucci, F. Beltram, H. E. Beere, E. H. Linfield, A. G. Davies, D. A. Ritchie, R. C. Iotti, and F. Rossi, "Terahertz semiconductor-heterostructure laser," *Nature* **417**, 156 (2002).
- L. Bosco, M. Franckić, G. Scalari, M. Beck, A. Wacker, and J. Faist, "Thermoelectrically cooled THz quantum cascade laser operating up to 210 K," *Appl. Phys. Lett.* **115**, 010601 (2019).
- M. A. Kainz, M. P. Semtsiv, G. Tsianos, S. Kurlov, W. T. Masselink, S. Schönhuber, H. Detz, W. Schrenk, K. Unterrainer, G. Strasser, and A. M. Andrews, "Thermoelectric-cooled terahertz quantum cascade lasers," *Opt. Express* **27**, 20688 (2019).
- A. Khalatpour, A. K. Paulsen, C. Deimert, Z. R. Wasilewski, and Q. Hu, "High-power portable terahertz laser systems," *Nat. Photonics* **15**, 16 (2021).
- Y. Leng Lim, P. Dean, M. Nikolić, R. Kliese, S. P. Khanna, M. Lachab, A. Valavanis, D. Indjin, Z. Ikonić, P. Harrison, E. H. Linfield, A. Giles Davies, S. J. Wilson, and A. D. Rakić, "Demonstration of a self-mixing displacement sensor based on terahertz quantum cascade lasers," *Appl. Phys. Lett.* **99**, 081108 (2011).
- A. D. Rakić, T. Taimre, K. Bertling, Y. L. Lim, P. Dean, D. Indjin, Z. Ikonić, P. Harrison, A. Valavanis, S. P. Khanna, M. Lachab, S. J. Wilson, E. H. Linfield,

- and A. G. Davies, "Swept-frequency feedback interferometry using terahertz frequency QCLs: A method for imaging and materials analysis," *Opt. Express* **21**, 22194 (2013).
- ⁹T. Taimre, M. Nikolić, K. Bertling, Y. L. Lim, T. Bosch, and A. D. Rakić, "Laser feedback interferometry: A tutorial on the self-mixing effect for coherent sensing," *Adv. Opt. Photonics* **7**, 570 (2015).
- ¹⁰A. Rakić, T. Taimre, K. Bertling, Y. Lim, P. Dean, A. Valavanis, and D. Indjin, "Sensing and imaging using laser feedback interferometry with quantum cascade lasers," *Appl. Phys. Rev.* **6**, 021320 (2019).
- ¹¹R. A. Lewis, "A review of terahertz detectors," *J. Phys. D: Appl. Phys.* **52**, 433001 (2019).
- ¹²Y. L. Lim, K. Bertling, T. Taimre, T. Gillespie, C. Glenn, A. Robinson, D. Indjin, Y. Han, L. Li, E. H. Linfield, A. G. Davies, P. Dean, and A. D. Rakić, "Coherent imaging using laser feedback interferometry with pulsed-mode terahertz quantum cascade lasers," *Opt. Express* **27**, 10221 (2019).
- ¹³P. Dean, Y. L. Lim, A. Valavanis, R. Kliese, M. Nikolić, S. P. Khanna, M. Lachab, D. Indjin, Z. Ikonić, P. Harrison, A. D. Rakić, E. H. Linfield, and A. G. Davies, "Terahertz imaging through self-mixing in a quantum cascade laser," *Opt. Lett.* **36**, 2587–2589 (2011).
- ¹⁴Y. Ren, R. Wallis, D. S. Jessop, R. Degl'Innocenti, A. Klimont, H. E. Beere, and D. A. Ritchie, "Fast terahertz imaging using a quantum cascade amplifier," *Appl. Phys. Lett.* **107**, 011107 (2015).
- ¹⁵T. Hagelschuer, M. Wienold, H. Richter, L. Schrottke, K. Biermann, H. T. Grahn, and H.-W. Hübers, "Terahertz gas spectroscopy through self-mixing in a quantum-cascade laser," *Appl. Phys. Lett.* **109**, 191101 (2016).
- ¹⁶S. Han, K. Bertling, P. Dean, J. Keeley, A. D. Burnett, Y. L. Lim, S. P. Khanna, A. Valavanis, E. H. Linfield, A. Giles Davies, D. Indjin, T. Taimre, and A. D. Rakić, "Laser feedback interferometry as a tool for analysis of granular materials at terahertz frequencies: Towards imaging and identification of plastic explosives," *Sensors* **16**, 352 (2016).
- ¹⁷Y. L. Lim, T. Taimre, K. Bertling, P. Dean, D. Indjin, A. Valavanis, S. P. Khanna, M. Lachab, H. Schaidler, T. W. Prow, H. Peter Soyer, S. J. Wilson, E. H. Linfield, A. Giles Davies, and A. D. Rakić, "High-contrast coherent terahertz imaging of porcine tissue via swept-frequency feedback interferometry," *Biomed. Opt. Express* **5**, 3981–3989 (2014).
- ¹⁸X. Qi, K. Bertling, T. Taimre, G. Agnew, Y. L. Lim, T. Gillespie, A. Robinson, M. Brünig, A. Demić, P. Dean, L. H. Li, E. H. Linfield, A. G. Davies, D. Indjin, and A. D. Rakić, "Observation of optical feedback dynamics in single-mode terahertz quantum cascade lasers: Transient instabilities," *Phys. Rev. A* **103**, 033504 (2021).
- ¹⁹F. P. Mezzapesa, L. L. Columbo, M. Brambilla, M. Dabbicco, S. Borri, M. S. Vitiello, H. E. Beere, D. A. Ritchie, and G. Scamarcio, "Intrinsic stability of quantum cascade lasers against optical feedback," *Opt. Express* **21**, 13748 (2013).
- ²⁰L. L. Columbo and M. Brambilla, "Multimode regimes in quantum cascade lasers with optical feedback," *Opt. Express* **22**, 10105 (2014).
- ²¹A. Demić, Z. Ikonić, P. Dean, and D. Indjin, "Dual resonance phonon–photon–phonon terahertz quantum-cascade laser: Physics of the electron transport and temperature performance optimization," *Opt. Express* **28**, 38788 (2020).
- ²²G. Agnew, A. Grier, T. Taimre, Y. L. Lim, K. Bertling, Z. Ikonić, A. Valavanis, P. Dean, J. Cooper, S. P. Khanna, M. Lachab, E. H. Linfield, A. G. Davies, P. Harrison, D. Indjin, and A. D. Rakić, "Model for a pulsed terahertz quantum cascade laser under optical feedback," *Opt. Express* **24**, 20554 (2016).
- ²³M. Wienold, L. Schrottke, M. Giehler, R. Hey, W. Anders, and H. T. Grahn, "Low-voltage terahertz quantum-cascade lasers based on LO-phonon-assisted interminiband transitions," *Electron. Lett.* **45**, 1030 (2009).
- ²⁴N. W. Almond, X. Qi, R. Degl'Innocenti, S. J. Kindness, W. Michailow, B. Wei, P. Braeuninger-Weimer, S. Hofmann, P. Dean, D. Indjin *et al.*, "External cavity terahertz quantum cascade laser with a metamaterial/graphene optoelectronic mirror," *Appl. Phys. Lett.* **117**, 041105 (2020).
- ²⁵X. Qi, G. Agnew, T. Taimre, S. Han, Y. L. Lim, K. Bertling, A. Demić, P. Dean, D. Indjin, and A. D. Rakić, "Laser feedback interferometry in multi-mode terahertz quantum cascade lasers," *Opt. Express* **28**, 14246–14262 (2020).
- ²⁶L. L. Columbo, M. Brambilla, F. P. Mezzapesa, M. Dabbicco, and G. Scamarcio, "Quantum cascade lasers with optical feedback: Regular multimode dynamics," *Proc. SPIE* **9370**, 937013 (2015).
- ²⁷N. N. Vukovic, J. V. Radovanovic, V. B. Milanovic, A. V. Antonov, D. I. Kuritsyn, V. V. Vaks, and D. L. Boiko, "Regular self-pulsations in external cavity mid-IR quantum cascade lasers," *arXiv:1902.00205* (2019).
- ²⁸T. Heil, I. Fischer, W. Elsässer, and A. Gavrielides, "Dynamics of semiconductor lasers subject to delayed optical feedback: The short cavity regime," *Phys. Rev. Lett.* **87**, 243901 (2001).
- ²⁹I. Kundu, F. Wang, X. Qi, H. Nong, P. Dean, J. R. Freeman, A. Valavanis, G. Agnew, A. T. Grier, T. Taimre, L. Li, D. Indjin, J. Mangeney, J. Tignon, S. S. Dhillon, A. D. Rakić, J. E. Cunningham, E. H. Linfield, and A. G. Davies, "Ultrafast switch-on dynamics of frequency-tuneable semiconductor lasers," *Nat. Commun.* **9**, 3076 (2018).
- ³⁰A. Mottaghizadeh, D. Gacemi, P. Laffaille, H. Li, M. Amanti, C. Sirtori, G. Santarelli, W. Hänsel, R. Holzgart, L. H. Li, E. H. Linfield, and S. Barbieri, "5-ps-long terahertz pulses from an active-mode-locked quantum cascade laser," *Optica* **4**, 168 (2017).
- ³¹F. Wang, V. Pistore, M. Riesch, H. Nong, P.-B. Vigneron, R. Colombelli, O. Parillaud, J. Mangeney, J. Tignon, C. Jiruschek, and S. S. Dhillon, "Ultrafast response of harmonic modelocked THz lasers," *Light: Sci. Appl.* **9**, 51 (2020).
- ³²S. Biasco, H. E. Beere, D. A. Ritchie, L. Li, A. G. Davies, E. H. Linfield, and M. S. Vitiello, "Frequency-tunable continuous-wave random lasers at terahertz frequencies," *Light: Sci. Appl.* **8**, 43 (2019).